Optical Coherence Tomography: A Review

16

Tawimas Shaipanich, Hamid Pahlevaninezhad, and Stephen Lam

Introduction

Globally, lung cancer is the most common cause of cancer deaths with over 1.6 million deaths per year [1]. Adenocarcinoma is the predominant cell type among women. In men, aside from a few European countries, such as France, Spain, and the Netherlands, adenocarcinoma has surpassed squamous cell carcinoma as the predominant cell type [2]. The shift in lung cancer cell types from the more centrally located squamous cell and small cell carcinomas to the more peripherally located adenocarcinomas, as well as smaller lesions detected by thoracic CT, necessitates a change in the approach to bronchoscopic diagnosis of peripheral lung lesions that are generally beyond the range of a standard flexible bronchoscope ≥3 cm in outer diameter. Radial probe endobronchial ultrasound with or without an electromagnetic navigation or virtual bronchoscopy navigation system improves the diagnostic yield from an average of 34% to 69% [3–7]. This is lower than CT-guided transthoracic lung biopsy with a diagnostic yield ≥80% even for lesions ≤2 cm [8, 9]. In the context of a CT lung cancer screening program, only 20–34% of the screening CT-detected lung cancers are diagnosed by bronchoscopy (Table 16.1) [10, 11] and unpublished data). Although endoscopic biopsy has a lower complication rate in pneumothorax and bleeding than CT-guided transthoracic lung biopsy [8, 9, 12, 13], improvement in the accuracy of endoscopic biopsy for small peripheral lung lesions is needed if bronchoscopy is going to play a major role in lung cancer diagnosis. For centrally located bronchial cancers that are not visible by CT, it is often difficult to differentiate between in situ carcinoma and invasive carcinoma. The ability to diagnose the depth of tumor invasion can guide therapy. In this chapter, the role of optical coherence tomography (OCT), Doppler OCT, polarization-sensitive OCT (PS-OCT), and autofluorescence OCT in the diagnosis of lung cancer and the potential application in nonmalignant lung diseases are discussed.

T. Shaipanich, MD, FRCPC
H. Pahlevaninezhad, MD, PhD
S. Lam, MD, FRCPC (✉)
Cancer Imaging Unit, Integrative Oncology Department, British Columbia Cancer Agency Research Centre, 675 West 10th Avenue, Vancouver, BC, Canada, V5Z 1L3

The University of British Columbia, Vancouver, BC, Canada
e-mail: slam2@bccancer.bc.ca

History and Historical Perspective

Optical coherence tomography (OCT) was originally developed for noninvasive cross-sectional imaging of biological systems [14, 15]. This optical imaging method offers near histologic resolution for visualizing cellular and extracellular structures at and below the tissue surface up to

J.P. Díaz-Jimenez, A.N. Rodriguez (eds.), *Interventions in Pulmonary Medicine*,
https://doi.org/10.1007/978-3-319-58036-4_16

Table 16.1 Mode of diagnosis and accuracy for screening CT-detected lung cancers

Modality	NLST		PanCan	
	Diagnostic method (%)	Positive rate (%)	Diagnostic method (%)	Positive rate (%)
Bronchoscopy	34	55.5	20	55.6
CT-FNA/core	19	66.5	38	81.1
Surgery	47	73.9	42	77.6

CT computed tomography, *FNA* fine needle transthoracic lung biopsy, *NLST* National Lung Screening Trial, *PanCan* Pan-Canadian Early Detection of Lung Cancer Study

2–3 mm. The utility of this imaging modality was first demonstrated in ophthalmology and cardiology [16, 17]. It was later developed as an optical imaging and biopsy tool in other organs such as the esophagus and lung [18–21].

OCT is similar to B-mode ultrasound. Instead of sound waves, light waves are used for imaging. Optical interferometry is used to detect the light that is scattered or reflected by the tissue to generate a one-dimensional tissue profile along the light direction. By scanning the light beam over the tissue, two-dimensional images or three-dimensional volumetric images can be recorded. For bronchoscopic application, the imaging procedure is performed using fiber-optic probes that can be miniaturized to enable imaging of airways down to the terminal bronchiole. These probes can be inserted down the instrument channel during standard bronchoscopic examination under conscious sedation. The axial and lateral resolutions of OCT range from approximately 5 to 30 μm, and the imaging depth is 2–3 mm depending on the imaging conditions. This combination of resolution and imaging depth is ideal for examining changes originating in epithelial tissues such as airways. Unlike ultrasound, light does not require a liquid coupling medium and thus is more compatible with airway imaging. There are no associated risks from the weak near-infrared light sources that are used for OCT.

In time domain OCT, a depth-resolved line profile of tissue is obtained by measuring the autocorrelation function [14, 22] using a low-coherence time light source and an interferometer comprised of a variable-length reflective reference arm and a sample arm where the tissue is illuminated. A signal is generated when the path length of light scattered from a particular tissue depth matches that from the reference arm. In frequency domain OCT, the spectral density function is measured to obtain a depth-resolved optical scattering of the tissue through Fourier transformation. The spectral density function can be measured with interferometers using either a broadband light source and a spectrometer or a wavelength-swept light source and a square-law detector. This approach was shown to provide orders of magnitude enhancement in detection sensitivity compared to time domain OCT [23–27].

In Doppler OCT, the energy of photons from a moving system is transformed according to the four-vector momentum and the Lorentz transformation. According to the special theory of relativity, the energy of photons emitted from an object moving relative to an observer is transformed the same way leading to different energies compared to those seen by an observer that is stationary relative to the photon source. These different energies that correlate with different frequencies are called Doppler effect that can be used to detect moving sources by measuring a change in the frequency of the optical field emitted from the source. The OCT signal contains the information about the phase of the optical field scattered from a tissue sample. Therefore, moving objects can be detected by evaluating frequency shifts in their OCT signals [28, 29]. This technique can be used to visualize pulmonary vasculature in vivo during endoscopic imaging [30]. Doppler signals are created by analyzing the OCT data stream using the Kasai velocity estimator to evaluate the Doppler phase shift between A-scans in each frame. Endoscopic Doppler OCT can be difficult due to the motion artifacts such as from cardiac pulsations and

breathing movement. Bulk tissue motion correction algorithms are used to reduce artifacts.

Polarization-sensitive OCT (PS-OCT) is another extension to OCT to improve detailed tissue differentiation. By analyzing the polarization state of backscattered light, PS-OCT can provide information about tissue birefringence, diattenuation, optical axis orientation, and depolarization. Using PS-OCT, highly organized, anisotropic tissue layers such as muscles, bones, and blood vessel walls can be identified by their innate birefringence. Clinical applications of PS-OCT have been demonstrated in the determination of burn depth in vivo [31], the measurement of collagen and smooth muscle cell content in atherosclerotic plaques [32], the differentiation of benign lesions from malignant lesions in the larynx [33], and the detection of nerve fiber bundle loss in glaucoma [34, 35]. Obtaining polarization-dependent optical properties of tissue with PS-OCT entails two essential requirements. Firstly, the incident light on the tissue needs to have known polarization states (commonly circular polarization) [36, 37] or multiple sequential polarization states (not necessarily known) with defined polarization relation between them [38, 39]. Secondly, the polarization state of light scattered from tissue needs to be detected using a polarization diversity detection scheme. Polarization-sensitive detection can also be used to reduce the effects of polarization in structural OCT imaging that uses rotary probes. As the spinning fiber-optic probe is continuously flexing and in motion, the polarization state of the light exiting the tip of the probe is constantly varying, creating artificial intensity variations during OCT imaging. These variations can be significantly reduced using polarization diversity detection [40].

A recent advance in OCT imaging is co-registered autofluorescence OCT (AF-OCT) [41]. Autofluorescence imaging makes use of fluorescence and absorption properties to provide information about the biochemical composition and metabolic state of endogenous fluorophores in tissues [42, 43]. Most endogenous fluorophores are associated with the tissue matrix or are involved in cellular metabolism. The most important fluorophores are structural proteins such as collagen and elastin and those involved in cellular metabolism such as nicotinamide adenine dinucleotide (NADH) and flavins [43]. Upon illumination by violet or blue light (380–460 nm), normal tissues fluoresce strongly in the green (480–520 nm). Malignant tissues have a markedly reduced and redshifted autofluorescence signal due to the breakdown of extracellular matrix components as well as increased absorption by blood. These differences have been exploited to detect preinvasive and invasive bronchial cancers in central airways [44]. AF-OCT overcomes the limitation of autofluorescence bronchoscopy because the OCT imaging probes are much smaller than flexible video bronchoscopes allowing access to small peripheral airways beyond bronchoscopic view. AF-OCT allows rapid scanning of airway vasculature less prone to motion artifacts compared to Doppler OCT [45].

Endoscopic AF-OCT System

Figure 16.1 illustrates the components of an AF-OCT prototype system is shown in Fig. 1, and an AF-OCT prototype is shown in Fig. 16.1. A Mach-Zehnder interferometer driven by a wavelength-swept source comprises the OCT subsystem (Fig. 16.2a). The AF subsystem uses a 445 nm excitation laser and a photomultiplier tube for the detection of autofluorescence emission. Endoscopic imaging of airways is implemented using fiber-optic catheters that scan in a rotational manner using proximal motors. A large-scale motor actuates the rotor of a fiber-optic rotary joint (FORJ) that is connected to an imaging catheter, enabling proximally driven rotational scans of the catheter's fiber assembly. The imaging catheter consists of a double-clad fiber (DCF) catheter. This fiber assembly is fixed inside a torque cable that transfers rotational and pullback motions from the proximal end to the distal end (Fig. 16.2b). The rotating assembly is placed inside a close-ended 900 μm diameter stationary plastic tube if the catheter is going to be reused.

In one configuration (Fig. 16.2b), the AF excitation light is coupled to the DCF inner

Fig. 16.1 Illustrates the components of an AF-OCT prototype system

cladding [41], and in another system configuration (Fig. 16.2c), the AF excitation light is coupled to the DCF core using fused fiber components [46–48] and a custom-designed FORJ [49]. The latter allows a tightly focused AF excitation light that exits the catheter, enabling higher-resolution AF imaging.

Preclinical Studies

Ex vivo studies have shown that OCT can visualize structural features in airways, adjacent alveoli, and pulmonary nodules that correspond closely to the histopathology (Fig. 16.3) [20, 50–54]. The basement membrane can be clearly seen between the epithelial and submucosal layer. Cartilage usually appears as darker signal-poor regions due to its low scattering properties. OCT measurements of mean luminal diameter, inner luminal area, airway wall area, and percent airway wall thickness prior to surgical resection were found to correlate significantly with the histology down to the ninth-generation bronchi in the resected specimens [55].

Clinical Studies

Endoscopic OCT imaging is performed during flexible bronchoscopy under local anesthesia applied to the upper airways and conscious sedation [21, 56]. The OCT probe can be inserted inside a guide sheath similar to radial endobronchial ultrasound through the working channel of the bronchoscope into the targeted airways. When clinically indicated, following removal of the catheter, histological and/or cytological samples are collected. OCT imaging adds about 5–10 min to the standard procedure time. It is usually well tolerated by patients. Repeat OCT measurements of airways were found to be reproducible and hence can be used for longitudinal assessment of changes in airway morphology [57].

Lung Cancer

The ability of OCT to discern invasive cancer versus CIS or dysplasia was investigated [21]. Normal or hyperplasia is characterized by one or two cell layers above a highly scattering basement membrane and upper submucosa. As the epithelium changes from normal/hyperplasia to metaplasia, various grades of dysplasia, and CIS, the thickness of the epithelial layer increases; quantitative measurement of the epithelial thickness showed that invasive carcinoma is significantly thicker than carcinoma in situ ($p = 0.004$) and dysplasia is significantly thicker than metaplasia or hyperplasia ($p = 0.002$). The nuclei become more readily visible in high-grade dysplasia or CIS. The basement membrane is still intact in CIS but became discontinuous or

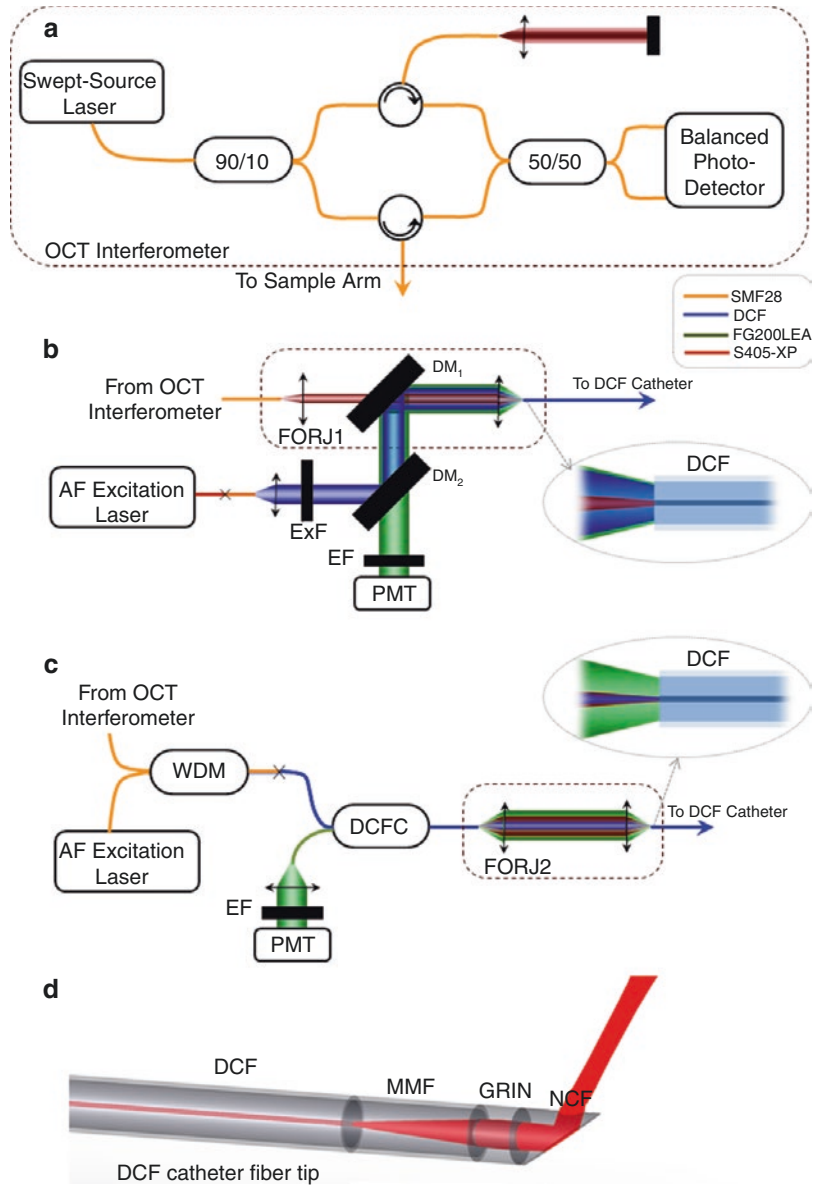

Fig. 16.2 Schematic diagram of OCT and AF-OCT. (**a**) OCT, (**b**) inner cladding AFI excitation, (**c**) core AFI excitation subsystems, and (**d**) optical elements at the tip of the DCF catheter. *DM* dichroic mirror, *ExF* excitation filter, *EF* emission filter, *PMT* photomultiplier, *WDM* wavelength division multiplexer, *DCFC* double-clad fiber coupler, *FORJ* fiber-optic rotary joint, *DCF* double-clad fiber, *MMF* (step-index) multimode fiber, *GRIN* graded index fiber, *NCF* no-core fiber

no longer visible with invasive cancer [21]. Squamous cell carcinoma has different OCT features than adenocarcinoma [52, 53] (Fig. 16.4).

The morphology of the peripheral lung nodules has been characterized. Lung parenchyma can be identified by the presence of signal-void alveolar spaces that appear as a honeycomb-like structure. Pulmonary nodule is identified by replacement of alveoli with solid tissue [45, 58, 59]. Adenocarcinomas with lepidic growth pattern are recognized by their thickened alveolar walls [45] (Fig. 16.4). After OCT interpretation training sessions, clinicians can diagnose common primary lung cancers (adenocarcinoma, squamous cell carcinoma, and poorly differentiated carcinoma) with an average accuracy of 82.6% (range 73.7–94.7%) [60]. Although OCT cannot replace histology in the diagnosis of lung carcinoma, it has the potential to aid in diagnosing lung carcinomas as a complement to tissue biopsy, particularly when insufficient tissue is available for pathology assessment. OCT may be

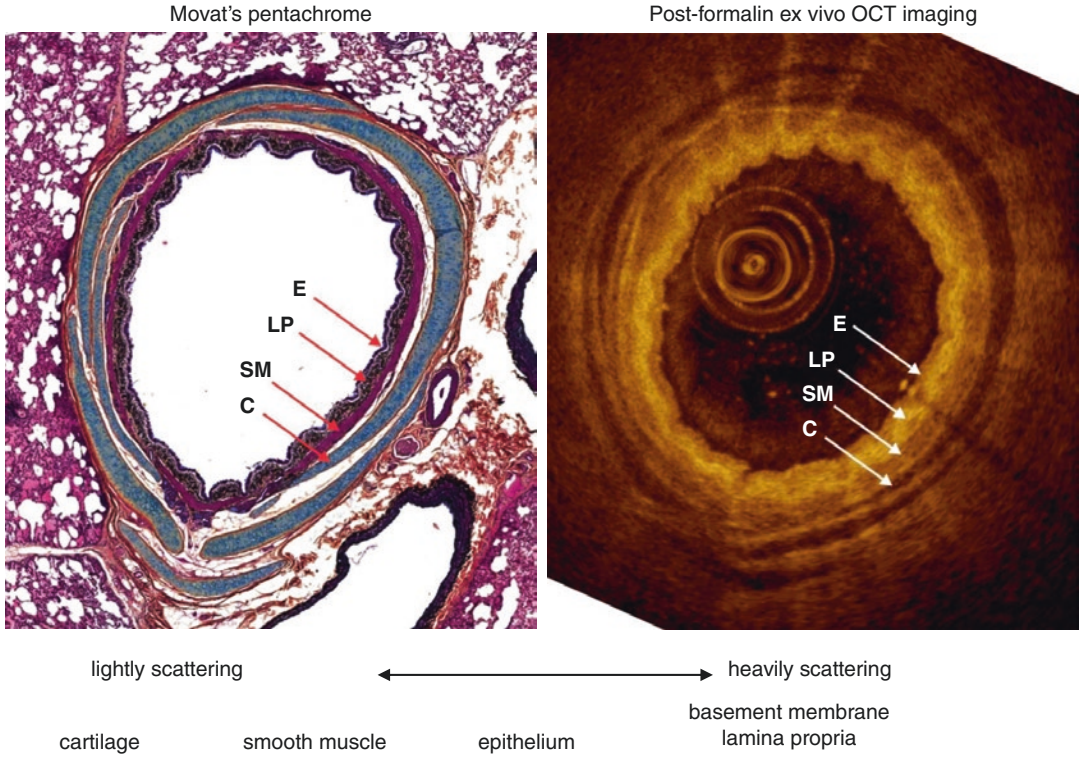

Fig. 16.3 Correlation of OCT image with histopathology in porcine airway. *Black* = nuclei, elastic fibers; *yellow* = collagen, reticular fibers; *blue* = ground substance, mucin; *bright red* = fibrin; *red* = muscle

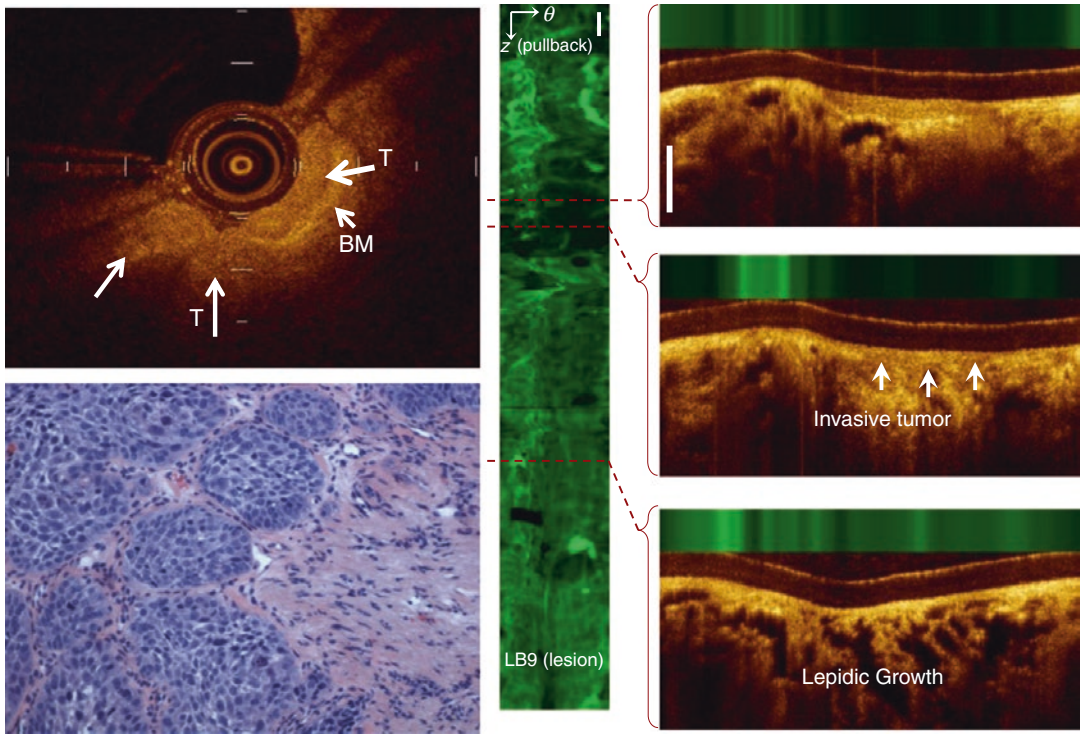

Fig. 16.4 (**a**) OCT and histological image of a squamous cell carcinoma showing the in situ component and invasion through the basement membrane (*arrows*). (**b**) AF-OCT of an adenocarcinoma with lepidic growth. In the AF image, there is a loss of green autofluorescence

useful for confirming the nature of the lesion before taking a biopsy. Since OCT probes can be miniaturized, they can be inserted inside biopsy needles/catheters to guide biopsy under real time without removing the imaging probe from a guide sheath and reinserting the biopsy forceps or needle with the possibility of displacement or migration to a different airway [56].

Asthma

It is known that asthma phenotypes are heterogeneous and influence the response to treatment. Bronchial thermoplasty (BT) is a non-pharmacologic method to treat patients with chronic persistent asthma [61]. Currently, there is no method to select patients who will benefit from BT. OCT imaging was performed in two patients with chronic persistent steroid-dependent asthma prior to and immediately after bronchial thermoplasty as well as at 3 weeks, 6 weeks, 6 months, and 2 years after bronchial thermoplasty. Prior to BT, distinct asthma phenotypes were observed between the patient (patient A) who had sustained benefit from BT for over 2 years and the one who did not (patient B) (Fig. 16.5) [62]. PS-OCT [36, 63, 64] that can define highly organized tissue layers such as smooth muscle and collagen may be a useful non-biopsy tool to study the effect of pharmacologic and non-pharmacologic therapies.

Chronic Obstructive Pulmonary Disease

Chronic obstructive pulmonary disease (COPD) is a heterogeneous disease characterized by both small airway and parenchymal abnormalities. There is increasing evidence to suggest that these two morphologic phenotypes, although related, may have different clinical presentations, prognosis, and therapeutic responses to medications. A recent ex vivo study using micro-CT showed that narrowing and disappearance of small conducting airways occur prior to the onset of emphysematous destruction and that these changes can explain the increased peripheral airways resistance reported in COPD [65]. Clinical CT using an acceptable dose of radiation provides airway images up to the fifth generation. Unfortunately, the resolution of CT is not adequate to image critical events that begin at the seventh branching generation nor can it measure morphological changes in different layers of the airway wall. OCT can overcome this limitation with small optical probes that can image airways

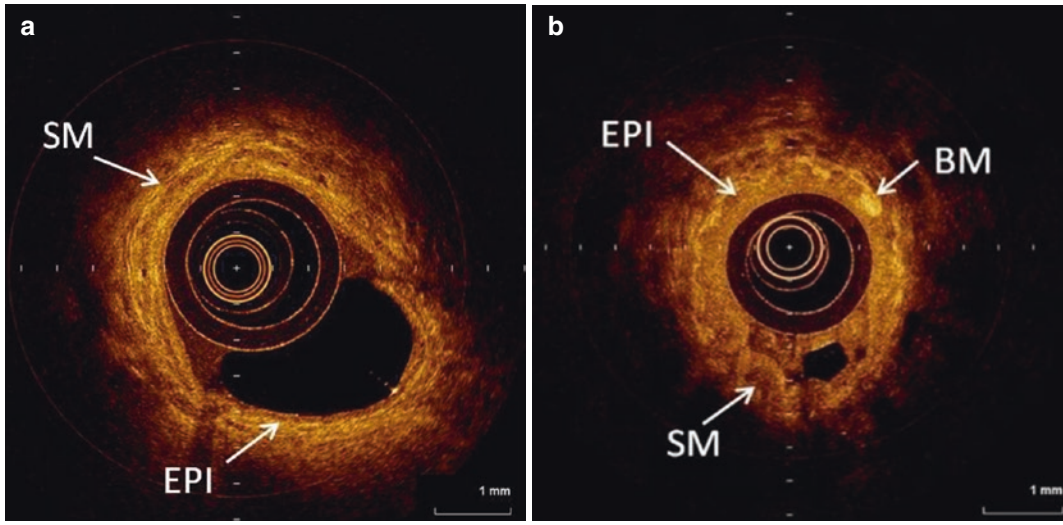

Fig. 16.5 OCT images of two patients before bronchial thermoplasty (BT) illustrating different phenotypic features. (**a**) Long-term responder following BT; (**b**) nonresponder with BT. *EPI* epithelium, *BM* basement membrane, *SM* smooth muscle

as small as terminal bronchioles with high resolution [55, 65, 66]. Coxson et al. compared OCT measurements with CT scans and lung function in COPD patients [67]. In 44 current and former smokers, OCT imaging was used to measure the airway dimensions in specific bronchial segments. These data were compared with CT measurements of the exact same airway using a three-dimensional reconstruction of the airway tree (Pulmonary Workstation 2.0; VIDA Diagnostics, Inc., Iowa City, IA). A strong correlation between CT and OCT measurements of lumen and wall area was observed. The correlation between FEV_1%-predicted and CT- and OCT-measured wall area (as percentage of the total area) of fifth-generation airways was good for both imaging modalities, but the slope of the relationship was much steeper using OCT than using CT, indicating greater sensitivity of OCT in detecting changes in wall measurements that relate to FEV_1. They concluded that OCT is more sensitive for discriminating the changes in the more distal airways of subjects with a range of expiratory airflow obstruction compared with CT. In addition to airway wall remodeling, alveolar wall destruction in COPD can also be clearly visualized using OCT with the emphysematous alveoli appearing as large voids compared with the small alveoli seen in those with normal lung function [53] (Fig. 16.6).

Sex differences in airway remodeling in COPD have also been investigated using OCT to help understand why women have a 50% increased risk of COPD compared with men after adjustment for the amount of smoking. Female human smokers have significantly thicker airway walls compared to male human smokers similar to the changes in a mouse model of COPD [68].

Airway and Lumen Calibration

Airway diameter measurement via bronchoscopy is not reliable due to optical distortion of the bronchoscope lens that varies among bronchoscopes and limited ability to gauge depth. Respiratory motions interfere with airway measurement. Airway measurement can be performed using CT scans. However, real-time examination is not always available, and radiation exposure is a concern. Using phantoms, excised pig airways, and in vivo human airways during bronchoscopy, Williamson et al. demonstrated that airway measurements using anatomic OCT are accurate and reliable and compare favorably with CT imaging [69]. OCT was used to measure airway diameter in patients with subglottic tracheal stenosis, main bronchial stenosis, and tracheomalacia. The real-time OCT information was found to be helpful for determining the length of the stenosis, extent of tumor involvement beyond the bronchoscopic view, and severity of the tracheomalacia or guide the choice of airway stent. The investigators conclude anatomic OCT with conventional bronchoscopy

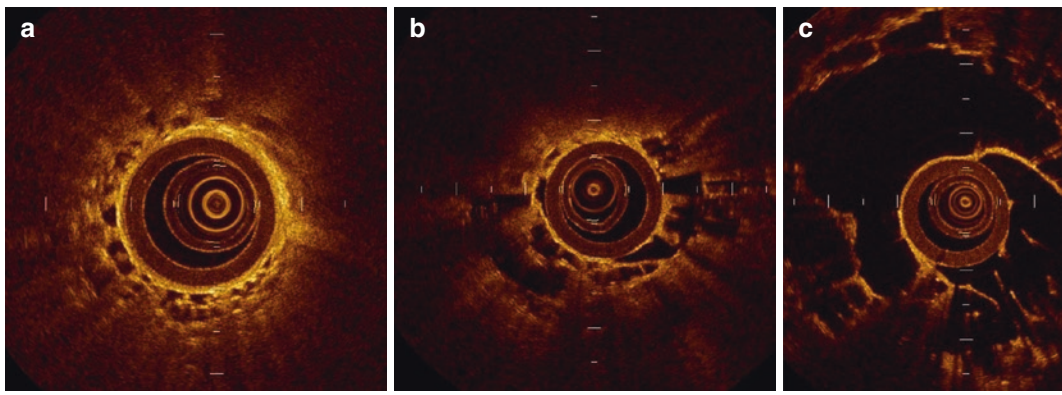

Fig. 16.6 OCT image of terminal bronchiole and adjacent alveoli. (**a**) Normal bronchiole; (**b**) patient with moderate emphysema; (**c**) patient with severe dysplasia showing progressive destruction of alveolar walls

allows accurate real-time airway measurements and may assist bronchoscopic assessment [70].

Obstructive Sleep Apnea

Changing of the upper airway sizes during sleep is the key pathophysiologic change in patient with obstructive sleep apnea (OSA). Reduction in pharyngeal size correlates with increased sleep disorder breathing and degree of nocturnal desaturation [71]. CT scan has been used to measure the upper airway size. However, measuring upper airway dimension during sleep and awake with CT is not practical plus concern with radiation exposure. Anatomic OCT offers a real-time quantitative measurement of the upper airway shape and size during sleep or awake comparable to CT scan [72]. Individuals with OSA were found to have a smaller velopharyngeal cross-sectional area than BMI-, gender-, and age-matched control volunteers, but comparable shape suggesting it is an abnormality in size rather than shape that is the more important anatomical predictor of OSA [73].

Future Applications

The ability to image the bronchial vasculature down to 12 μm diameter in 5–7 cm airway segments during bronchoscopy along with structural information using AF-OCT (Fig. 16.7) enables comparison of vasculature in normal and abnormal airways. The ability to visualize detailed vascular networks could provide opportunities to study angiogenesis to differentiate benign from malignant lung nodules, characterize biological

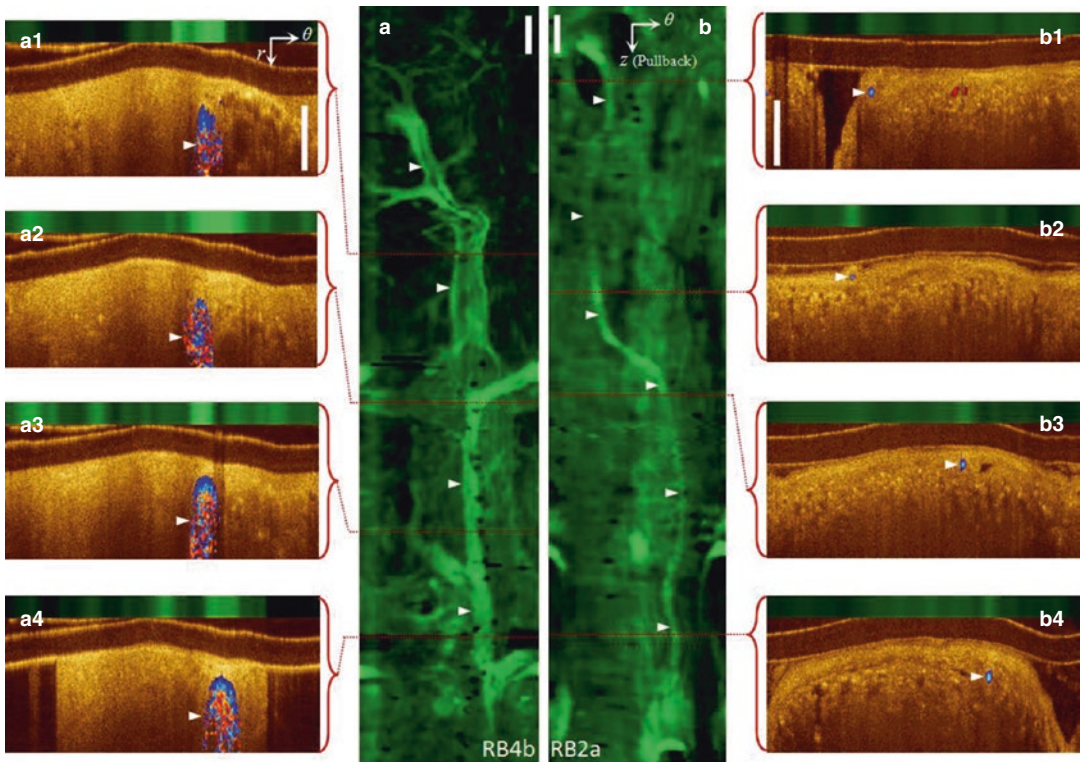

Fig. 16.7 Bronchial vasculature detection by AF-OCT with validation by Doppler OCT. (**a**) A large blood vessel running parallel to the airway (RB4b) with several smaller branching vessels is clearly visualized in the AF image. Doppler OCT (a_1–a_4) confirms these structures as blood vessels. (**b**) Another example of smaller airway blood vessels identified by AF-OCT confirmed by Doppler-OCT. (b_1–b_4) Small vessels down to 12 μm in diameter are visualized by dark lumen in the magnified image. White scale bars are 1 mm

aggressiveness of lung cancer, study vascular remodeling in different lung diseases such as COPD and asthma [74–76], and improve safety of cryobiopsy by avoiding biopsy of larger blood vessels. AF-OCT may provide the means to monitor rejection following lung transplantation. The effect of therapy in patients with pulmonary fibrosis can be studied by PS-OCT that can characterize collagen and elastin [59].

Summary

OCT, PS-OCT, Doppler OCT, and AF-OCT provide unprecedented opportunity to provide high-resolution structural and functional information on airway and lung tissue that cannot be otherwise obtained by other imaging modalities such as CT or MRI. In the central airways, it can differentiate in situ from invasive squamous cell carcinoma to guide therapy. In the peripheral lung, it has the potential to diagnose peripheral lung nodules, to guide biopsy in real time with improved accuracy and safety, as well as to study the effect of pharmacologic and non-pharmacologic therapies. It is a minimally invasive procedure that can be performed in conjunction with standard flexible bronchoscopy under conscious sedation. It has tremendous potential to be integrated into pulmonary medicine as a standard diagnostic procedure.

References

1. Fitzmaurice C, Dicker D, Pain A, Hamavid H, Moradi-Lakeh M, MacIntyre MF, et al. The global burden of cancer 2013. JAMA Oncol. 2015;1(4):505–27. Epub 2015/07/17
2. Lortet-Tieulent J, Soerjomataram I, Ferlay J, Rutherford M, Weiderpass E, Bray F. International trends in lung cancer incidence by histological subtype: adenocarcinoma stabilizing in men but still increasing in women. Lung Cancer. 2014;84(1):13–22. Epub 2014/02/15
3. Schreiber G, McCrory DC. Performance characteristics of different modalities for diagnosis of suspected lung cancer: summary of published evidence. Chest. 2003;123(1 Suppl):115S–28S. Epub 2003/01/16
4. Wang Memoli JS, Nietert PJ, Silvestri GA. Meta-analysis of guided bronchoscopy for the evaluation of the pulmonary nodule. Chest. 2012;142(2):385–93. Epub 2011/10/08
5. Chen A, Chenna P, Loiselle A, Massoni J, Mayse M, Misselhorn D. Radial probe endobronchial ultrasound for peripheral pulmonary lesions. A 5-year institutional experience. Ann Am Thorac Soc. 2014;11(4):578–82. Epub 2014/03/19
6. Eberhardt R, Kahn N, Gompelmann D, Schumann M, Heussel CP, Herth FJ. LungPoint--a new approach to peripheral lesions. J Thorac Oncol. 2010;5(10):1559–63. Epub 2010/08/31
7. Ost DE, Ernst A, Lei X, Kovitz KL, Benzaquen S, Diaz-Mendoza J, et al. Diagnostic yield and complications of bronchoscopy for peripheral lung lesions. Results of the AQuIRE registry. Am J Respir Crit Care Med. 2016;193(1):68–77. Epub 2015/09/15
8. Kothary N, Lock L, Sze DY, Hofmann LV. Computed tomography-guided percutaneous needle biopsy of pulmonary nodules: impact of nodule size on diagnostic accuracy. Clin Lung Cancer. 2009;10(5):360–3. Epub 2009/10/08
9. Heyer CM, Reichelt S, Peters SA, Walther JW, Muller KM, Nicolas V. Computed tomography-navigated transthoracic core biopsy of pulmonary lesions: which factors affect diagnostic yield and complication rates? Acad Radiol. 2008;15(8):1017–26. Epub 2008/07/16
10. Church TR, Black WC, Aberle DR, Berg CD, Clingan KL, Duan F, et al. Results of initial low-dose computed tomographic screening for lung cancer. N Engl J Med. 2013;368(21):1980–91. Epub 2013/05/24
11. Aberle DR, DeMello S, Berg CD, Black WC, Brewer B, Church TR, et al. Results of the two incidence screenings in the National Lung Screening Trial. N Engl J Med. 2013;369(10):920–31. Epub 2013/09/06
12. Wiener RS, Schwartz LM, Woloshin S, Welch HG. Population-based risk for complications after transthoracic needle lung biopsy of a pulmonary nodule: an analysis of discharge records. Ann Intern Med. 2011;155(3):137–44. Epub 2011/08/04
13. Steinfort DP, Khor YH, Manser RL, Irving LB. Radial probe endobronchial ultrasound for the diagnosis of peripheral lung cancer: systematic review and meta-analysis. Eur Respir J. 2011;37(4):902–10. Epub 2010/08/10
14. Fujimoto JG, De Silvestri S, Ippen EP, Puliafito CA, Margolis R, Oseroff A. Femtosecond optical ranging in biological systems. Opt Lett. 1986;11(3):150. Epub 1986/03/01
15. Youngquist RC, Carr S, Davies DE. Optical coherence-domain reflectometry: a new optical evaluation technique. Opt Lett. 1987;12(3):158–60. Epub 1987/03/01
16. Huang D, Swanson EA, Lin CP, Schuman JS, Stinson WG, Chang W, et al. Optical coherence tomography. Science. 1991;254(5035):1178–81.
17. Tearney GJ, Brezinski ME, Boppart SA, Bouma BE, Weissman N, Southern JF, et al. Images in cardiovascular medicine. Catheter-based optical imaging of a human coronary artery. Circulation. 1996;94(11):3013. Epub 1996/12/01

18. Fujimoto JG, Brezinski ME, Tearney GJ, Boppart SA, Bouma B, Hee MR, et al. Optical biopsy and imaging using optical coherence tomography. Nat Med. 1995;1(9):970–2.
19. Tearney GJ, Brezinski ME, Bouma BE, Boppart SA, Pitris C, Southern JF, et al. In vivo endoscopic optical biopsy with optical coherence tomography. Science. 1997;276(5321):2037–9.
20. Tsuboi M, Hayashi A, Ikeda N, Honda H, Kato Y, Ichinose S, et al. Optical coherence tomography in the diagnosis of bronchial lesions. Lung Cancer. 2005;49(3):387–94.
21. Lam S, Standish B, Baldwin C, McWilliams A, leRiche J, Gazdar A, et al. In vivo optical coherence tomography imaging of preinvasive bronchial lesions. Clin Cancer Res. 2008;14(7):2006–11. Epub 2008/04/03
22. Fercher AF, Mengedoht K, Werner W. Eye-length measurement by interferometry with partially coherent light. Opt Lett. 1988;13(3):186–8. Epub 1988/03/01
23. Choma M, Sarunic M, Yang C, Izatt J. Sensitivity advantage of swept source and Fourier domain optical coherence tomography. Opt Express. 2003;11(18):2183–9. Epub 2003/09/08
24. de Boer JF, Cense B, Park BH, Pierce MC, Tearney GJ, Bouma BE. Improved signal-to-noise ratio in spectral-domain compared with time-domain optical coherence tomography. Opt Lett. 2003;28(21):2067–9. Epub 2003/11/01
25. Leitgeb R, Hitzenberger C, Fercher A. Performance of fourier domain vs. time domain optical coherence tomography. Opt Express. 2003;11(8):889–94. Epub 2003/04/21
26. Wojtkowski M, Bajraszewski T, Targowski P, Kowalczyk A. Real-time in vivo imaging by high-speed spectral optical coherence tomography. Opt Lett. 2003;28(19):1745–7. Epub 2003/09/30
27. Yun SH, Tearney GJ, de Boer JF, Iftimia N, Bouma BE. High-speed optical frequency-domain imaging. Opt Express. 2003;11(22):2953–63.
28. Izatt JA, Kulkarni MD, Yazdanfar S, Barton JK, Welch AJ. In vivo bidirectional color Doppler flow imaging of picoliter blood volumes using optical coherence tomography. Opt Lett. 1997;22(18):1439–41. Epub 2008/01/12
29. Yang V, Gordon M, Qi B, Pekar J, Lo S, Seng-Yue E, et al. High speed, wide velocity dynamic range Doppler optical coherence tomography (part I): system design, signal processing, and performance. Opt Express. 2003;11(7):794–809. Epub 2003/04/07
30. Lee AMD, Ohtani K, MacAulay C, McWilliams A, Shaipanich T, Yang VXD, et al. In vivo lung microvasculature visualized in three dimensions using fiber-optic color Doppler optical coherence tomography. J Biomed Opt. 2013;18(5):50501.
31. Park BH, Saxer C, Srinivas SM, Nelson JS, de Boer JF. In vivo burn depth determination by high-speed fiber-based polarization sensitive optical coherence tomography. J Biomed Opt. 2001;6(4):474–9. Epub 2001/12/01
32. Nadkarni SK, Pierce MC, Park BH, de Boer JF, Whittaker P, Bouma BE, et al. Measurement of collagen and smooth muscle cell content in atherosclerotic plaques using polarization-sensitive optical coherence tomography. J Am Coll Cardiol. 2007;49(13):1474–81. Epub 2007/04/03
33. Burns JA, Kim KH, deBoer JF, Anderson RR, Zeitels SM. Polarization-sensitive optical coherence tomography imaging of benign and malignant laryngeal lesions: an in vivo study. Otolaryngol Head Neck Surg. 2011;145(1):91–9. Epub 2011/04/16
34. Braaf B, Vermeer KA, de Groot M, Vienola KV, de Boer JF. Fiber-based polarization-sensitive OCT of the human retina with correction of system polarization distortions. Biomed Opt Express. 2014;5(8):2736–58. Epub 2014/08/20
35. Zotter S, Pircher M, Torzicky T, Baumann B, Yoshida H, Hirose F, et al. Large-field high-speed polarization sensitive spectral domain OCT and its applications in ophthalmology. Biomed Opt Express. 2012;3(11):2720–32. Epub 2012/11/20
36. Hee MR, Huang D, Swanson EA, Fujimoto JG. Polarization-sensitive low-coherence reflectometer for birefringence characterization and ranging. J Opt Soc Am B. 1992;9(6):903–8.
37. deBoer JF, Milner TE, vanGemert MJC, Nelson JS. Two-dimensional birefringence imaging in biological tissue by polarization-sensitive optical coherence tomography. Opt Lett. 1997;22(12):934–6.
38. Kim KH, Park BH, YP T, Hasan T, Lee B, Li JA, et al. Polarization-sensitive optical frequency domain imaging based on unpolarized light. Opt Express. 2011;19(2):552–61.
39. Baumann B, Choi W, Potsaid B, Huang D, Duker JS, Fujimoto JG. Swept source/Fourier domain polarization sensitive optical coherence tomography with a passive polarization delay unit. Opt Express. 2012;20(9):10229–41.
40. Lee AM, Pahlevaninezhad H, Yang VX, Lam S, MacAulay C, Lane P. Fiber-optic polarization diversity detection for rotary probe optical coherence tomography. Opt Lett. 2014;39(12):3638–41. Epub 2014/07/01
41. Pahlevaninezhad H, Lee AMD, Shaipanich T, Raizada R, Cahill L, Hohert G, et al. A high-efficiency fiber-based imaging system for co-registered autofluorescence and optical coherence tomography. Biomed Opt Express. 2014;5(9):2978–87.
42. Lam S. The role of autofluorescence bronchoscopy in diagnosis of early lung cancer. In: Hirsch F, Bunn P, Kato H, et al., editors. IASLC textbook for prevention and detection of early lung cancer. London: Taylor & Francis; 2006. p. 149–58.
43. Wagnieres G, McWilliams A, Lung SL. Cancer imaging with fluorescence endoscopy. In: Mycek MA, Pogue BW, editors. Handbook of biomedical fluorescence. New York: CRC Press; 2003. p. 361–96.
44. McWilliams A, Shaipanich T, Lam S. Fluorescence and navigational bronchoscopy. Thorac Surg Clin. 2013;23(2):153–61. Epub 2013/04/10

45. Pahlevaninezhad H, Lee AM, Ritchie A, Shaipanich T, Zhang W, Ionescu DN, et al. Endoscopic Doppler optical coherence tomography and autofluorescence imaging of peripheral pulmonary nodules and vasculature. Biomed Opt Express. 2015;6(10):4191–9.
46. Madore WJ, De Montigny E, Ouellette O, Lemire-Renaud S, Leduc M, Daxhelet X, et al. Asymmetric double-clad fiber couplers for endoscopy. Opt Lett. 2013;38(21):4514–7. Epub 2013/11/02
47. Lorenser D, Yang X, Kirk RW, Quirk BC, McLaughlin RA, Sampson DD. Ultrathin side-viewing needle probe for optical coherence tomography. Opt Lett. 2011;36(19):3894–6. Epub 2011/10/04
48. Scolaro L, Lorenser D, Madore WJ, Kirk RW, Kramer AS, Yeoh GC, et al. Molecular imaging needle: dual-modality optical coherence tomography and fluorescence imaging of labeled antibodies deep in tissue. Biomed Opt Express. 2015;6(5):1767–81.
49. Pahlevaninezhad H, Lee AM, Hohert G, Lam S, Shaipanich T, Beaudoin E, et al. Endoscopic high-resolution autofluorescence imaging and OCT of pulmonary vascular networks. Opt Lett. 2016;41(14):3209–12.
50. Lee AM, Kirby M, Ohtani K, Candido T, Shalansky R, MacAulay C, et al. Validation of airway wall measurements by optical coherence tomography in porcine airways. PLoS One. 2014;9(6):e100145. Epub 2014/06/21
51. Hariri LP, Applegate MB, Mino-Kenudson M, Mark EJ, Bouma BE, Tearney GJ, et al. Optical frequency domain imaging of ex vivo pulmonary resection specimens: obtaining one to one image to histopathology correlation. J Vis Exp. 2013; 22(71). pii:3855. doi:10.3791/3855.
52. Hariri LP, Applegate MB, Mino-Kenudson M, Mark EJ, Medoff BD, Luster AD, et al. Volumetric optical frequency domain imaging of pulmonary pathology with precise correlation to histopathology. Chest. 2013;143(1):64–74. Epub 2012/03/31
53. Ohtani K, Lee AM, Lam S. Frontiers in bronchoscopic imaging. Respirology. 2012;17(2):261–9. Epub 2011/12/01
54. Pahlevaninezhad H, Lee AM, Lam S, MacAulay C, Lane PM. Coregistered autofluorescence-optical coherence tomography imaging of human lung sections. J Biomed Opt. 2014;19(3):36022. Epub 2014/04/02
55. Chen Y, Ding M, Guan WJ, Wang W, Luo WZ, Zhong CH, et al. Validation of human small airway measurements using endobronchial optical coherence tomography. Respir Med. 2015;109(11):1446–53. Epub 2015/10/03
56. Tan KM, Shishkov M, Chee A, Applegate MB, Bouma BE, Suter MJ. Flexible transbronchial optical frequency domain imaging smart needle for biopsy guidance. Biomed Opt Express. 2012;3(8):1947–54. Epub 2012/08/10
57. Kirby M, Ohtani K, Nickens T, Lisbona RM, Lee AM, Shaipanich T, et al. Reproducibility of optical coherence tomography airway imaging. Biomed Opt Express. 2015;6(11):4365–77. Epub 2015/11/26
58. Hariri LP, Mino-Kenudson M, Applegate MB, Mark EJ, Tearney GJ, Lanuti M, et al. Toward the guidance of transbronchial biopsy: identifying pulmonary nodules with optical coherence tomography. Chest. 2013;144(4):1261–8. Epub 2013/07/06
59. Hariri LP, Villiger M, Applegate MB, Mino-Kenudson M, Mark EJ, Bouma BE, et al. Seeing beyond the bronchoscope to increase the diagnostic yield of bronchoscopic biopsy. Am J Respir Crit Care Med. 2013;187(2):125–9. Epub 2013/01/17
60. Hariri LP, Mino-Kenudson M, Lanuti M, Miller AJ, Mark EJ, Suter MJ. Diagnosing lung carcinomas with optical coherence tomography. Ann Am Thorac Soc. 2015;12(2):193–201. Epub 2015/01/07
61. Trivedi A, Pavord ID, Castro M. Bronchial thermoplasty and biological therapy as targeted treatments for severe uncontrolled asthma. Lancet Respir Med 2016;4(7):585–92. Review.
62. Kirby M, Ohtani K, Lopez Lisbona RM, Lee AM, Zhang W, Lane P, et al. Bronchial thermoplasty in asthma: 2-year follow-up using optical coherence tomography. Eur Respir J. 2015;46(3):859–62.
63. De Boer J, Srinivas S, Malekafzali A, Chen Z, Nelson J. Imaging thermally damaged tissue by polarization sensitive optical coherence tomography. Opt Express. 1998;3(6):212–8. Epub 1998/09/14
64. Everett MJ, Schoenenberger K, Colston BW Jr, Da Silva LB. Birefringence characterization of biological tissue by use of optical coherence tomography. Opt Lett. 1998;23(3):228–30. Epub 2007/12/18
65. McDonough JE, Yuan R, Suzuki M, Seyednejad N, Elliott WM, Sanchez PG, et al. Small-airway obstruction and emphysema in chronic obstructive pulmonary disease. N Engl J Med. 2011;365(17):1567–75. Epub 2011/10/28
66. Coxson HO, Mayo J, Lam S, Santyr G, Parraga G, Sin DD. New and current clinical imaging techniques to study chronic obstructive pulmonary disease. Am J Respir Crit Care Med. 2009;180(7):588–97. Epub 2009/07/18
67. Coxson HO, Lam S. Quantitative assessment of the airway wall using computed tomography and optical coherence tomography. Proc Am Thorac Soc. 2009;6(5):439–43. Epub 2009/08/19
68. Tam A, Churg A, Wright JL, Zhou S, Kirby M, Coxson HO, et al. Sex differences in airway remodeling in a mouse model of chronic obstructive pulmonary disease. Am J Respir Crit Care Med. 2016;193(8):825–34.
69. Williamson JP, Armstrong JJ, McLaughlin RA, Noble PB, West AR, Becker S, et al. Measuring airway dimensions during bronchoscopy using anatomical optical coherence tomography. Eur Respir J. 2010;35(1):34–41. Epub 2009/06/23
70. Williamson JP, McLaughlin RA, Phillips MJ, Armstrong JJ, Becker S, Walsh JH, et al. Using optical coherence tomography to improve diagnostic and therapeutic bronchoscopy. Chest. 2009;136(1):272–6.
71. Haponik EF, Smith PL, Bohlman ME, Allen RP, Goldman SM, Bleecker ER. Computerized tomogra-

phy in obstructive sleep apnea. Correlation of airway size with physiology during sleep and wakefulness. Am Rev Respir Dis. 1983;127(2):221–6. Epub 1983/02/01
72. Armstrong JJ, Leigh MS, Sampson DD, Walsh JH, Hillman DR, Eastwood PR. Quantitative upper airway imaging with anatomic optical coherence tomography. Am J Respir Crit Care Med. 2006;173(2):226–33.
73. Walsh JH, Leigh MS, Paduch A, Maddison KJ, Philippe DL, Armstrong JJ, et al. Evaluation of pharyngeal shape and size using anatomical optical coherence tomography in individuals with and without obstructive sleep apnoea. J Sleep Res. 2008;17(2):230–8.
74. Carmeliet P, Jain RK. Angiogenesis in cancer and other diseases. Nature. 2000;407(6801):249–57. Epub 2000/09/23
75. McDonald DM. Angiogenesis and remodeling of airway vasculature in chronic inflammation. Am J Respir Crit Care Med. 2001;164(10 Pt 2):S39–45. Epub 2001/12/06
76. Jeffery PK. Structural and inflammatory changes in COPD: a comparison with asthma. Thorax. 1998;53(2):129–36. Epub 1998/06/13